JOC The Journal of Organic Chemistry

Article

pubs.acs.org/joc

Influence of Pendant Chiral C^{γ}-(Alkylideneamino/Guanidino) Cationic Side-chains of PNA Backbone on Hybridization with Complementary DNA/RNA and Cell Permeability

Deepak R. Jain,[†] Libi Anandi V,[‡] Mayurika Lahiri,[‡] and Krishna N. Ganesh*,[†]

[†]Chemical Biology Unit, Indian Institute of Science Education and Research, Dr Homi Bhabha Road, Pune 411008, Maharashtra, India

[‡]Biological Sciences, Indian Institute of Science Education and Research, Dr Homi Bhabha Road, Pune 411008, Maharashtra, India

Supporting Information

ABSTRACT: Intrinsically cationic and chiral C^{γ}-substituted peptide nucleic acid (PNA) analogues have been synthesized in the form of $\gamma(S)$-ethyleneamino (*eam*)- and $\gamma(S)$-ethyl-eneguanidino (*egd*)-PNA with two carbon spacers from the backbone. The relative stabilization (ΔT_m) of duplexes from modified cationic PNAs as compared to 2-aminoethylglycyl (*aeg*)-PNA is better with complementary DNA (PNA:DNA) than with complementary RNA (PNA:RNA). Inherently, PNA:RNA duplexes have higher stability than PNA:DNA duplexes, and the guanidino PNAs are superior to amino PNAs. The cationic PNAs were found to be specific toward their complementary DNA target as seen from their significantly lower binding with DNA having single base mismatch. The differential binding avidity of cationic PNAs was assessed by the displacement of DNA duplex intercalated ethidium bromide and gel electrophoresis. The live cell imaging of amino/guanidino PNAs demonstrated their ability to penetrate the cell membrane in 3T3 and MCF-7 cells, and cationic PNAs were found to be accumulated in the vicinity of the nuclear membrane in the cytoplasm. Fluorescence-activated cell sorter (FACS) analysis of cell permeability showed the efficiency to be dependent upon the nature of cationic functional group, with guanidino PNAs being better than the amino PNAs in both cell lines. The results are useful to design new biofunctional cationic PNA analogues that not only bind RNA better but also show improved cell permeability.

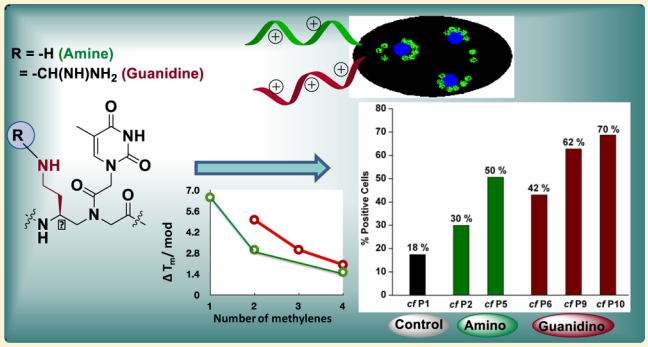

INTRODUCTION

Peptide nucleic acids[1,2] are effective DNA analogues in which the chiral sugar−phosphate backbone is replaced with an achiral pseudopeptide backbone consisting of 2-aminoethyl-glycyl (*aeg*) linkage (Figure 1a). The nucleobases (A/T/G/C) are attached through a methylene carbonyl linker to this backbone at the glycyl amino nitrogen via tertiary amide linkage. PNA hybridizes with complementary DNA/RNA via established Watson−Crick base pairing with greater affinity compared to equivalent DNA:DNA or DNA:RNA duplexes.[3,4] The higher binding affinity of PNA is partially due to the absence of negative charge and the higher flexibility in the backbone. PNAs, being neither peptide nor nucleic acids, possess resistance to both proteases and nucleases and consequently have a longer life span in the cellular environment.[5] The simplicity of chemical structure, ease of synthesis, and superior DNA/RNA complementation properties have made PNA an attractive gene regulatory agent.[3,6,7] However, the efficacy of PNA as an effective antisense/antigene agent has been hampered by its low aqueous solubility, ambiguity in binding orientation (parallel vs antiparallel), and poor cellular uptake.[8] To overcome these limitations many chemical modifications of PNA have been attempted, which have effected some improvements in PNA properties.[9−11]

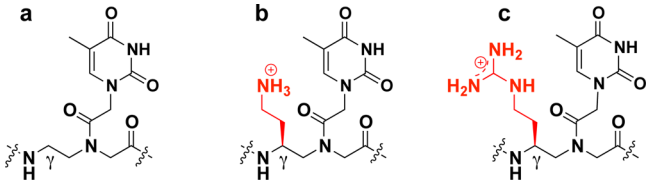

Figure 1. Chemical structures of (a) *aeg*-PNA, (b) γ-(*S-eam*) *aeg*-PNA, and (c) γ-(*S-egd*) *aeg*-PNA.

It has been shown that incorporation of D-lysine at the α-position has significantly improved the solubility of PNA oligomers in water and stabilized the derived PNA:DNA duplexes.[12] A recent crystallographic study of antiparallel mixed-sequence PNA−DNA decamer heteroduplex, compris-

Received: July 20, 2014
Published: September 15, 2014

Scheme 1. Synthesis of γ-(*S-eam*) and γ-(*S-egd*) Modified PNA Monomers

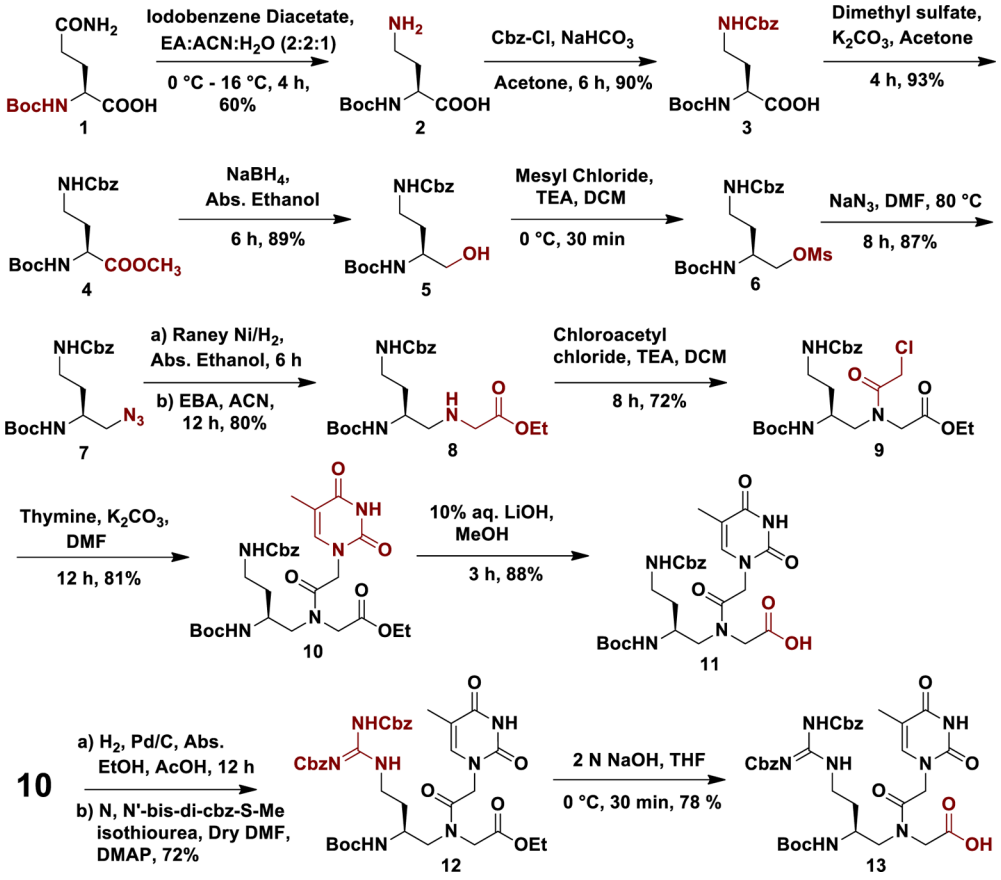

ing a "chiral box" of three-residues of D-lysine, provides evidence that introduction of a chiral center increases the rigidity of the polyamide backbone.[13,14] It has been demonstrated that PNAs incorporating the cationic guanidinium group in the side-chain at C^{α} (GPNA)[15] or C^{γ} (γGPNA)[16] on the backbone result in enhanced binding selectively to complementary RNA and DNA, respectively, and in addition enhance the cellular uptake of the PNAs. The chiral C^{γ} side-chain on the backbone is presumed to preorganize the PNA oligomer into a right-handed helix, thereby favoring its binding to complementary DNA/RNA.[16−18] PNA carrying a diethylene glycol side-chain at the C^{γ} site displayed better hybridization property and water solubility.[19] We have recently shown that C^{γ}-substituted PNAs bearing an azido group via methylene/butylene side-chains enhance the PNA:DNA hybrid stability and are useful to append fluorophores by click chemistry.[20]

Among PNA analogues bearing cationic functional groups like amine or guanidine on pendant side-chains on the backbone, systematic studies on the effect of alkyl spacers on DNA/RNA complementation is lacking. This motivated us to design, synthesize, and study PNAs incorporating a methylamino side-chain at the $C^{\alpha/\gamma}$ site on the backbone, which showed regio- and stereospecific dependence of PNA:DNA hybrid stability and cell-penetrating ability.[21,22] Continuing this objective, we now report studies on C^{γ}-substituted PNAs possessing ethyleneamino (*eam*) (Figure 1b) and ethyleneguanidino (*egd*) (Figure 1c) side-chains to determine the comparative effects of cationic groups and the intervening carbon chain length on the hybridization of PNAs to complementary DNA/RNA. It is demonstrated that the relative degree of stabilization observed for the PNA:DNA duplexes of cationic PNAs was higher compared to that of corresponding PNA:RNA, while the inherent avidity of cationic amine/guanidine modified PNAs was higher for complementary RNA. The cationic PNAs were found to efficiently permeate the NIH 3T3 and MCF-7 cells, with the C^{γ}-ethyleneguanidino PNAs being better than the C^{γ}-ethyleneamino PNAs.

RESULTS

Synthesis of C^{γ}-Ethyleneamino/Guanidino PNA Monomers. The synthesis of target PNA monomers (**11** and **13**) containing thymine nucleobase was started from the commercially available Boc-L-glutamine **1** (Scheme 1), which was subjected to Hoffman rearrangement[23] to obtain 4-amino-2-(*N*-Boc-amino)butanoic acid **2**. The side-chain amine was protected with Cbz-group to get the orthogonally protected 4-(Cbz-amino)-2-(Boc-amino)butanoic acid **3**, which was esterified using dimethyl sulfate to yield compound **4**, followed by reduction using $NaBH_4$ to yield the primary alcohol **5**. This was converted to its mesylate derivative **6**, which upon treatment with NaN_3 gave the azide **7**. The reduction of azide to primary amine by Raney/Ni followed by N-alkylation of the resulting amine using ethylbromo acetate proceeded to the *N*-alkylated compound **8**. Upon treatment with chloroacetyl chloride, **8** gave the chloro derivative **9**, which was treated subsequently with thymine to get the ester PNA monomer **10**. The hydrolysis of the ester with LiOH afforded the desired γ-(*S-eam*) *aeg*-PNA-T monomer **11**.

dx.doi.org/10.1021/jo501639m | J. Org. Chem. 2014, 79, 9567−9577

Table 1. PNA Oligomers Synthesized with Their Molecular Weights[a]

Entry	Oligomers	Sequences	Calcd MW	Obs MW
P1	*aeg* PNA	H-T T A C C T C A G T-LysNH$_2$ 1 2 3 4 5 6 7 8 9 10	2805.1750	2805.0652
P2	*eam*-t$_{2a}$ PNA	H-Tt$_a$ACCTCAGT-LysNH$_2$	2848.2172	2848.3081
P3	*eam*-t$_{6a}$ PNA	H-TTACCt$_a$CAGT-LysNH$_2$	2848.2172	2848.2515
P4	*eam*-t$_{10a}$ PNA	H-TTACCTCAGt$_a$-LysNH$_2$	2848.2172	2848.5977
P5	*eam*-t$_{2a,6a}$ PNA	H-Tt$_a$ACCt$_a$CAGT-LysNH$_2$	2913.2414[M + Na]$^+$	2913.3682
P6	*egd*-t$_{2\gamma}$ PNA	H-Tt$_\gamma$ACCTCAGT-LysNH$_2$	2913.8384[M + Na]$^+$	2917.2097
P7	*egd*-t$_{6\gamma}$ PNA	H-TTACCt$_\gamma$CAGT-LysNH$_2$	2913.8384[M + Na]$^+$	2917.1689
P8	*egd*-t$_{10\gamma}$ PNA	H-TTACCTCAGt$_\gamma$-LysNH$_2$	2890.2390	2890.6897
P9	*egd*-t$_{2\gamma,6\gamma}$ PNA	H-Tt$_\gamma$ACCt$_\gamma$CAGT-LysNH$_2$	2975.3030	2975.4937
P10	*egd*-t$_{2\gamma,6\gamma,10\gamma}$ PNA	H-Tt$_\gamma$ACCt$_\gamma$CAGt$_\gamma$-LysNH$_2$	3060.3670	3060.1923
cf P1	*aeg* PNA-*cf*	*cf*-TTACCTCAGT-LysNH$_2$	3163.2227	3163.5088
cf P2	*eam*-t$_{2a}$ PNA-*cf*	*cf*-Tt$_a$ACCTCAGT-LysNH$_2$	3206.2649	3208.2456
cf P5	*eam*-t$_{2a,6a}$ PNA-*cf*	*cf*-Tt$_a$ACCt$_a$CAGT-LysNH$_2$	3249.3071	3253.3552
cf P6	*egd*-t$_{2\gamma}$ PNA-*cf*	*cf*-Tt$_\gamma$ACCTCAGT-LysNH$_2$	3272.1389 [M + Na]$^+$	3276.4036
cf P9	*egd*-t$_{2\gamma,6\gamma}$ PNA-*cf*	*cf*-Tt$_\gamma$ACCt$_\gamma$CAGT-LysNH$_2$	3335.3200	3337.3982
cf P10	*egd*-t$_{2\gamma,6\gamma,10\gamma}$ PNA-*cf*	*cf*-Tt$_\gamma$ACCt$_\gamma$CAGt$_\gamma$-LysNH$_2$	3418.4147	3420.3511

[a]See the Supporting Information for mass spectra; red **t$_a$** = ethyleneamino (*eam*) modified PNA-T unit and red **t$_\gamma$** = ethyleneguanidino (*egd*) modified PNA-T unit.

For the synthesis of the corresponding guanidinium analogue γ-(*S*-*egd*) *aeg*-PNA-T monomer **13**, the Cbz-group in compound **10** was deprotected to get the free amine. It was guanidinylated using *N*,*N*′-bis-di-Cbz-*S*-Me-isothiourea to obtain the ester **12**, which was hydrolyzed with NaOH to afford the desired PNA monomer **13**. All the intermediates and the final compounds were characterized by spectroscopic (^{1}H and ^{13}C NMR, mass spectroscopy) and analytical data (Supporting Information).

Synthesis of PNA Oligomers. The modified PNA monomers **11** and **13** were incorporated into *aeg*-PNA mixmer sequence **P1** at different sites in single or multiple copies. The oligomers were synthesized by manual solid-phase peptide synthesis using *Boc*-chemistry protocol[24] on L-lysine-derivatized MBHA resin utilizing the standard HOBt−HBTU coupling procedure. At the end of the assembly, the Cbz protection on the C$^\gamma$ side-chain and the exocyclic amino group on A, G, and C nucleobases were concurrently removed by triflouroacetic acid (TFA)−trifluoromethanesulfonic acid (TFMSA),[25] which also cleaved the PNAs from the solid support. Various modified and unmodified *aeg*-PNA oligomers that were synthesized are listed in Table 1.

For cellular uptake studies, PNA oligomers were tagged with 5(6)-carboxyfluorescein at the N-terminus (***cf*P1**−***cf*P10**) during the solid-phase synthesis to visualize the PNAs inside the cells. All PNA oligomers were purified by reverse-phase high-performance liquid chromatography (HPLC) and characterized by matrix-assisted laser desorption ionization time-of-flight (MALDI-TOF) mass spectrometric data (see Supporting Information for HPLC and MALDI-TOF spectra).

Hybridization Studies. The comparative effects of cationic substitutions (amine/guanidine) on the ethylene side-chain at the C$^\gamma$ position of PNA on the thermal stability (T_m) of the composed duplex with complementary DNA/RNA were evaluated by temperature-dependent UV absorbance studies. The various modified PNAs **1**−**10** were annealed individually with antiparallel complementary DNA **1** or complementary RNA **1** to form the corresponding PNA:DNA/PNA:RNA duplexes. The sequence specificity of the modified PNA oligomers toward target DNA was also assessed from their ability to form duplexes with DNA **2** having a single base mismatch. The thermal stability results are presented in Table 2, and it is seen that the modified amino (**P2**−**P5**) and guanidino (**P6**−**P10**) PNAs enhance the stability of the corresponding PNA:DNA **1** duplexes significantly compared to that of the unmodified *aeg*-PNA **P1**. The level of enhancement is dependent on the nature (amine/guandine), site (N-/C-terminus or center), and number of modifications, with ΔT_m in the range 2.5−14 °C. The relative comparisons of differential thermal stabilities (ΔT_m) of duplexes with amino- and guanidino-modified PNAs compared with the control *aeg*-PNA **P1** are shown in Figure 2.

dx.doi.org/10.1021/jo501639m | J. Org. Chem. 2014, 79, 9567−9577

Table 2. UV−T_m (°C) Values of PNA:DNA and PNA:RNA Duplexes[a]

entry	oligomers	DNA 1 (ap)	DNA 2 (mm)	RNA 1 (ap)
P1	*aeg*-PNA **1**	43.4	37.4	58.2
P2	*eam*-t_{2a}-PNA **2**	47.3	36.7	58.2
P3	*eam*-t_{6a}-PNA **3**	47.1	35.0	57.2
P4	*eam*-t_{10a}-PNA **4**	49.2	36.2	59.6
P5	*eam*-$t_{2a,6a}$-PNA **5**	49.7	37.2	59.3
P6	*egd*-$t_{2\gamma}$-PNA **6**	45.9	35.4	55.3
P7	*egd*-$t_{6\gamma}$-PNA **7**	48.8	36.3	55.3
P8	*egd*-$t_{10\gamma}$-PNA **8**	52.0	37.0	61.2
P9	*egd*-$t_{2\gamma,6\gamma}$-PNA **9**	51.9	38.4	62.0
P10	*egd*-$t_{2\gamma,6\gamma,10\gamma}$-PNA **10**	57.4	38.9	63.0

[a]DNA **1** (ap; antiparallel) = 5′ACTGAGGTAA 3′; DNA **2** (mm; mismatch) = 5′ACTGCGGTAA 3′; RNA **1** (ap; antiparallel) = 5′ ACUGAGGUAA 3′. All samples were prepared in 10 mM sodium phosphate buffer containing 10 mM NaCl and 0.1 mM EDTA at 2 μM strand concentration each. The T_m's are accurate up to ±0.5 °C.

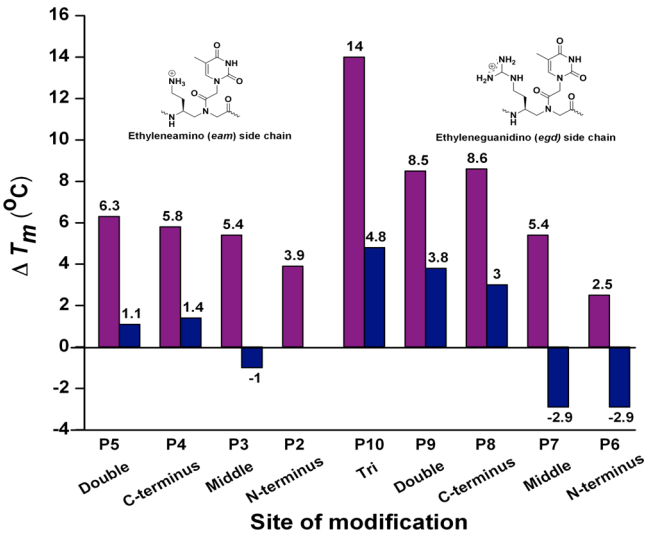

Figure 2. Comparative ΔT_m values for PNA:DNA and PNA:RNA duplexes formed by γ-(*S-eam*, **P2**−**P5**) and γ-(*S-egd*, **P6**−**P10**) over unmodified *aeg*-PNA at different positions on mixed decamer sequence with complementary DNA **1**, 5′ ACTGAGGTAA 3′, and complementary RNA **1**, 5′ ACUGAGGUAA 3′. ΔT_m indicates the difference in T_m with control *aeg*-PNA **1**. Red bars = PNA:DNA, and blue bars = PNA:RNA duplexes.

In the case of both amino and guanidino PNAs, modifications at C-terminus [γ-(*S-eam*) **P4**] and [γ-(*S-egd*) **P8**] stabilize the PNA:DNA duplexes (ΔT_m = 5.8 and 8.6 °C, respectively) better than the central (PNAs **P3**, ΔT_m = 3.7; and **P7**, ΔT_m= 5.4 °C) and N-terminus (**P2**, ΔT_m = 3.9; and **P6**, ΔT_m = 2.5 °C) modified PNAs. The degree of duplex stabilization is enhanced with an increase in the number of modifications in the sequence (**P5**, ΔT_m = 6.3; **P9**, ΔT_m = 8.5; and **P10**, ΔT_m = 14 °C), suggesting an average improvement in the duplex stability by ∼5 °C/modification for guanidino and ∼3 °C/modification for amino PNAs. The duplexes from guanidino-modified PNAs were always better stabilized than those of the amino-modified PNAs.

The higher binding affinity of cationic PNAs toward the negatively charged complementary DNA could arise from a generic electrostatic interaction between the two strands. To determine the sequence specificity, the modified PNAs were hybridized with DNA **2** having a single base mismatch in the middle of the sequence (Table 2). The introduction of one base-pair mismatch destabilized the control duplex PNA **P1**:DNA **2** by 6 °C. In comparison, the destabilization for mismatch duplexes from cationic amino- and guanidino-substituted PNA was significantly higher with ΔT_m's in the range −10 to −18.5 °C depending on the number of modifications. The guanidino PNAs showed more destabilization compared to the amino PNAs, and the higher mismatch duplex destabilization of cationic PNAs indicated their inherently superior sequence specificity toward target DNA, in addition to higher binding resulting from electrostatic interactions.

The cationic PNAs were examined for their capacities to hybridize complementary RNA, and the T_m's of the corresponding PNA:RNA duplexes are shown in Table 2. The amino (**P2**−**P5**)- and guanidino (**P6**−**P10**)-modified PNAs had a higher T_m for the derived PNA:RNA duplexes compared to their analogous PNA:DNA duplexes by ∼10 ± 0.5 °C. The degree of enhancement for cationic PNA:RNA duplexes over unmodified *aeg*-PNA:RNA duplexes was ∼3−5 °C, except for those from **P3**, **P6**, and **P7**, which actually showed destabilization.

Circular Dichroic Studies and Intercalator Displacement Assay. The structural effect of C$^\gamma$ side-chain substitution on the conformation of PNA:DNA and PNA:RNA duplexes was probed by circular dichroism (CD) spectroscopy. Although single-stranded PNA showed low-intensity CD signals, PNA:DNA/PNA:RNA complexes exhibit characteristic CD signatures because of the helicity induced by the chiral DNA/RNA in corresponding hybrids (Supporting Information). The PNA:DNA/RNA duplexes show two positive bands, one with moderate intensity between 260 and 270 nm and another of lower intensity between 218 and 225 nm accompanied by a negative band near 240 nm. No significant changes were seen in the CD profile of the duplexes from cationic PNAs compared to that of unmodified PNA **P1**, suggesting conformational similarity of all PNA:DNA and PNA:RNA duplexes.

The differential binding ability of the cationic PNAs toward complementary DNA was examined by their competence to displace the intercalated ethidium bromide (EtBr) from DNA:DNA duplex[26,27] (Supporting Information), monitored by reduced fluorescence emission intensity at 610 nm. The loss in fluorescence intensity is a consequence of strand invasion of DNA:DNA complex by PNA resulting in disassociation of the EtBr.[28] The extent and rate of displacement of intercalator bound to DNA:DNA duplex reflects the comparative abilities of *aeg*-PNA, γ-(*S-eam*)-PNA, and γ-(*S-egd*)-PNA to invade DNA:DNA duplex to form PNA:DNA duplex and is shown in Figure 3. The *aeg*-PNA **P1** displaced 84% of EtBr bound to DNA duplex as compared to ∼76% with C-terminus single amino-modified PNA **P4**. Interestingly, the analogous guanidino-modified cationic PNA **P8** was less effective with only 56% displacement efficiency in spite of having higher duplex stability. Further, the displacement efficiency did not noticeably depend on the number of amino and guanidino modifications in the PNA sequence (see Supporting Information). The EtBr displacing ability of amino-modified cationic PNA (**P4**) was found to be better than that of guanidino-modified PNA (**P8**) but less efficient than that of control *aeg*-PNA. It may be pointed out that the charge-neutral C$^\gamma$-methylene/butylene azido PNAs were more competent than either the amino or guanidino PNA analogues.[20] The lower efficiency of cationic

dx.doi.org/10.1021/jo501639m | J. Org. Chem. 2014, 79, 9567−9577

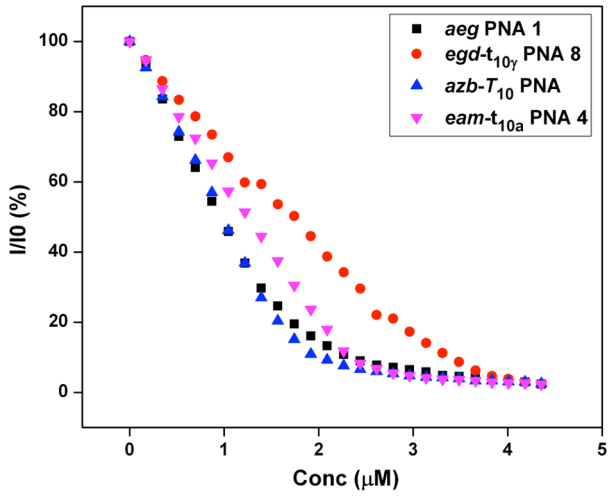

Figure 3. Comparative ethidium bromide displacement studies by different PNAs from ds-DNA (*azb*-T_{10} PNA = C$^{\gamma}$-substituted azidobutylene modified PNA).

PNAs in displacing EtBr from the DNA duplex is perhaps a consequence of retarded invasion due to electrostatic repulsion of their inherent positive charges from the positively charged EtBr, unlike that with neutral *aeg*-PNA or azido-PNA. Because of a lower pK_a of side-chain amino groups in *eam*-PNAs than that of guanidino function in *egd*-PNAs, they carry less positive charge at pH 7.0 and, hence, are better than guanidine PNAs in the displacement assay.

Electrophoretic Gel Mobility Shift Assay. The strand invasion of DNA duplex by cationic PNAs was demonstrated using electrophoretic mobility shift assay[29,30] using PNA **P10** as a representative example. Control *aeg*-PNA **P1** and the guanidino PNA **P10** were individually treated with complementary DNA **1**, and the complex formations were monitored by gel electrophoresis at ∼18 °C. The spots were visualized through shadowing by illuminating the gel placed on a fluorescent plate of silica gel F_{254} using UV light (Figure 4).

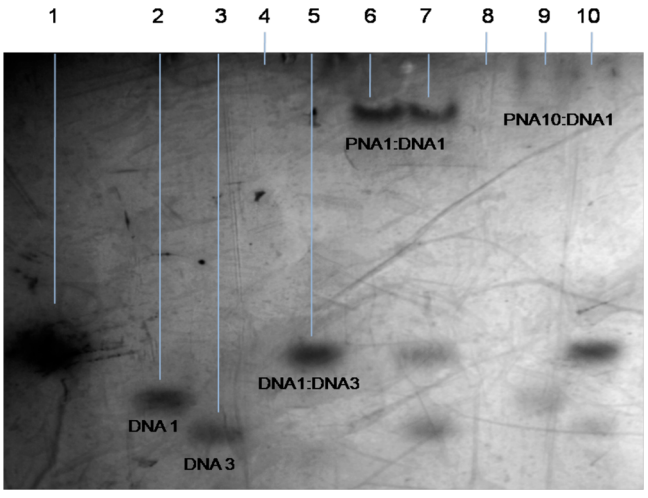

Figure 4. Electrophoretic mobility shift assay and competition binding experiment. Lane 1, Bromophenol blue; lane 2, DNA **1**; lane 3, DNA **3**; lane 4, PNA **P1**; lane 5, DNA **1**:DNA **3**; lane 6, PNA **P1**:DNA **1**; lane 7, DNA **1**:DNA **3** + PNA **P1**; lane 8, PNA **P10**; lane 9, PNA **10**:DNA **1**; lane 10, DNA **1**:DNA **3** + PNA **10** (DNA **1** = 5′ ACTGAGGTAA 3′; DNA **3** = 5′ TTACCTCAGT 3′).

The duplex DNA **1**:DNA **3** (lane 5) had retarded mobility compared to the single-stranded DNAs (lanes 2 and 3) due to its increased mass. Being negatively charged, single-stranded DNAs moved faster on gel while the neutral *aeg*-PNA **P1** (lane 4) and cationic PNA **P10** (lane 8) did not move out of the well. The reaction of PNA **P1** to duplex DNA **1**:DNA **3** results in strand-invaded product duplex **P1**:DNA **1**, liberating DNA **3** (lane 6). The **P1**:DNA **1** duplex is highly retarded in comparison with DNA duplex (lane 5) due to a reduced negative charge. The competition binding experiment was also carried out by adding cationic PNA **P10** to the DNA **1**:DNA **3** duplex, and the resultant products PNA **10**:DNA **1** duplex and the free DNA **3** were monitored on gel. In the cationic PNA **10**:DNA **1** duplex, the guanidino groups neutralize the negative charges on DNA, decreasing the net negative charge more than in **P1**:DNA **1** duplex, leading to retardation so much that it hardly moves out of the well (lane 9). The formation of PNA **P10**:DNA **1** duplex was also evident from the release of single-stranded DNA **3** and the appearance of retarded PNA:DNA complex (lane 10). These results suggest that the PNAs *aeg*-**P1** and the cationic **P10** invade the DNA **1**:DNA **3** duplex to form corresponding duplexes, displacing DNA **3**.

Cell Uptake Studies. The effects of cationic PNAs on their cell-penetrating abilities were investigated by treating NIH 3T3 and MCF-7 cell lines individually with the fluorescently labeled PNAs *aeg*-PNA (***cf*P1**), amino (***cf*P2** and ***cf*P5**) PNAs, and guanidino (***cf*P6**, ***cf*P9**, and ***cf*P10**) PNAs and visualization of their intracellular location by confocal microscopy. The live cells were incubated separately with the fluorescently labeled PNAs (1 μM) for 24 h and processed for visualization by laser scanning confocal microscope. Figure 5 shows confocal live cell images for the guanidino-modified PNA ***cf*P10** in NIH 3T3 and MCF-7 cells (see Supporting Information for images for other PNA oligomers). The images indicate that the cationic PNAs enter the cells and localize inside the cells around the nucleus irrespective of the site or type of modification and the cell line used. A definite qualitative proof for the PNA uptake by cells is seen from a superimposition of bright-field image (Figure 5A), Hoechst 33342 stained image (Figure 5B), and the green fluorescent image (Figure 5C) as shown in Figure 5D.

To quantitatively discern the cell-penetrating abilities of the various modified PNA oligomers, fluorescence activated cell sorter (FACS) analysis was performed as shown in Figure 6. In the case of C$^{\gamma}$-amino-modified PNAs (Figure 6A), the doubly modified amino-PNA ***cf*P5** showed a slightly higher mean fluorescence compared to the control PNA ***cf*P1** and PNA with single amino modification ***cf*P2**. The guanidino-modified PNAs followed a similar pattern with mean fluorescence intensities increasing with higher degree of substitution, in the order ***cf*P6**, ***cf*P9**, and ***cf*P10** (Figure 6B), all having higher fluorescence compared to PNA (***cf*P1**) and the amino PNA ***cf*P2**. The triply modified guanidino PNA ***cf*P10** showed the best fluorescence among all PNAs.

Although the mean fluorescence intensities of PNAs with different substitutions did not appear to vary too much, the percentage of positive cell counts (a measure of the percentage of the number of cells that have taken up the PNA inside that quantifies the cellular uptake of different modified PNAs) remarkably increased for the cationic amino- and guanidino-modified PNAs compared to unmodified *aeg*-PNA **P1** as shown in Figure 7. For control *aeg*-PNA (***cf*P1**), the percent positive cell count was ∼18%, while it increased to ∼30% for single amino modification (***cf*P2**) and to ∼50% for double amino

dx.doi.org/10.1021/jo501639m | J. Org. Chem. 2014, 79, 9567−9577

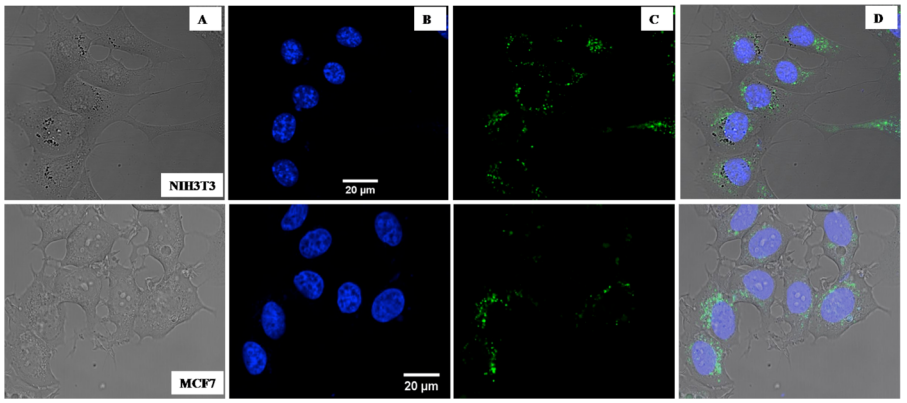

Figure 5. Distribution of three guanidino-modified PNA (***cf*P10**) inside NIH 3T3 and MCF-7 cells: (A) bright-field image, (B) Hoechst 33342 stained image, (C) green fluorescent image, and (D) superimposed image of A, B, and C.

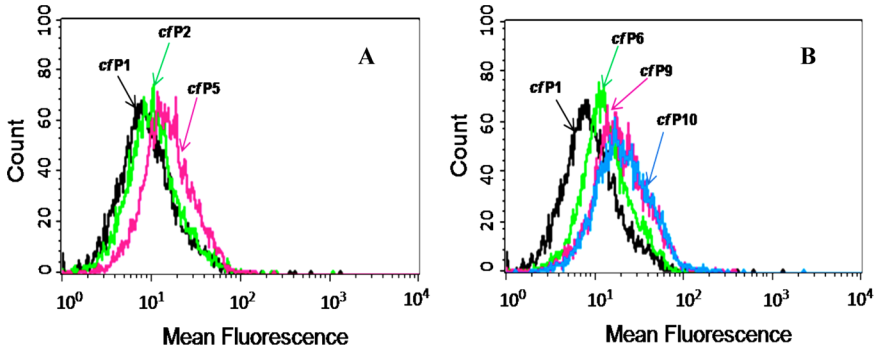

Figure 6. Quantitative estimation of cellular uptake in NIH 3T3 cells for (A) amino-modified PNAs and (B) guanidino-modified PNAs in comparison with control *aeg*-PNA by FACS analysis.

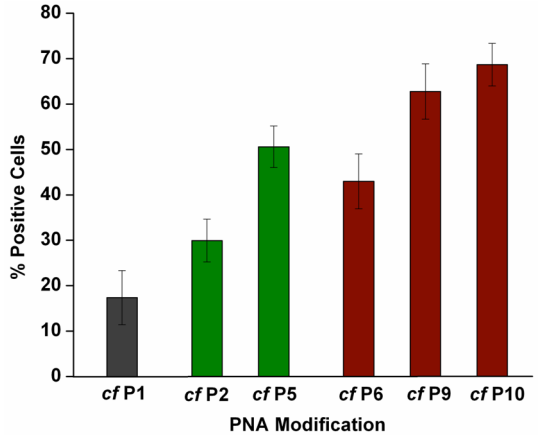

Figure 7. Percentage of positive cells count for various modified PNAs in NIH 3T3 cells by FACS analysis.

modifications (***cf*P5**), a 3-fold increase in the cell permeation compared to control PNA. The single guanidino modification (***cf*P6**) gave ∼42% positive cells, whereas for two guanidino modifications (***cf*P9**) the number of positive cells increased to ∼62%, which further increased to ∼70% for three guanidine-modified PNAs (***cf*P10**), thus amounting to a 4-fold increase in the cell penetration ability over that of unmodified PNA ***cf*P1**, clearly indicating an additive effect of cationic substitutions. The cytotoxicity of modified cationic PNAs was assessed by standard 3-(4,5-dimethylthiazol-2-yl)-2,5-diphenyltetrazolium bromide (MTT) assay, which showed >80% cell viability (untreated cells, 100%) for both unmodified and modified PNAs at different concentrations. The quantitative data for other PNA oligomers in both cell lines and the toxicity data are given in Supporting Information.

DISCUSSION

PNAs can be rendered cationic through modifications either in the backbone or conjugating a ligand through side-chains located at α- or γ-positions on the backbone. Of these, the γ-site has been shown to be versatile for modifications to effectively modulate the properties of PNA.[17,31,32] Continuing our efforts to tune the effective carbon chain length and charge on the cationic substitutions at C^{γ} of the PNA backbone, we studied PNA oligomers composed of C^{γ}-substituted 2-carbon spacer side-chain carrying multisite substitutions of amino and guanidino functions. These were synthesized from the amide L-glutamine by Hoffman rearrangement to yield amine followed by guanidination to finally enable PNA monomers bearing cationic functions (amino/guanidino) pendant on ethylene side-chain at $C^{\gamma}(S)$ of the PNA backbone. The cationic PNA oligomers incorporating these monomers at defined, multiple sites remarkably increased thermal stability of the derived PNA:DNA duplexes by 2.5−14 °C depending on the position and number of modified amino/guanidino units per PNA strand; further, the guanidino PNAs were better than amino PNAs, and both were much superior to unmodified PNA. The order of stabilization for amino PNA was C-terminus > N-terminus > middle, while that for guanidino PNA was C-terminus > middle > N-terminus; no definite reasoning can be attributed to these differences, although such positional effects are common with other analogues. The higher binding of

dx.doi.org/10.1021/jo501639m | *J. Org. Chem.* 2014, 79, 9567−9577

cationic PNAs is clearly due to both structural and electrostatic charge effects because a single base mismatch in the DNA sequence destabilized the duplex stability more than that with unmodified PNA. Thus, mere electrostatic interaction between the cationic PNA and the anionic DNA is not the only reason for stabilization of the duplex, and the cationic PNAs have better base sequence discriminating ability than standard PNA. The cationic PNA:RNA duplexes have significantly higher T_m compared to the analogous PNA:DNA duplexes, which assumes importance from an application perspective.

In electrophoretic experiments, the cationic PNAs retard the derived DNA duplex on gel as expected from a net negative charge reduction in the PNA:DNA duplex and demonstrated successful displacement of isosequential DNA from DNA:DNA duplex. However, the cationic PNA oligomers were less efficient (slower) compared to unmodified *aeg*-PNA in displacing the intercalated ethidium bromide from DNA:DNA duplex through strand invasion due to the ensuing PNA-intercalator cationic charge repulsion. The comparative ΔT_m °C/modification for PNA:DNA duplex collated from our work[21,22] and that of others[16,32,33] for $C^{\gamma}(S)$ substitution as a function of spacer methylenes and cation type is depicted in Table 3. It is seen that, for both amino and guanidino PNAs,

Table 3. Comparative ΔT_m °C/Modification in Thermal Stabilities of $C^{\gamma}(S)$-Substituted Cationic PNAs[a]

PNA-$(CH_2)_n$-X, $n\rightarrow$	1	2	3	4
X = amino	6.5	3	NR	1.7
X = guanidino	NR	5	3	2.0

[a]Values indicate the difference in T_m compared to analogous control *aeg*-PNA; NR, not reported.

ΔT_m °C/modification decreases with the increase in the number of carbons in the spacer chain. The results have thrown light on the structure activity relationship on the role of spacer in determining the thermal stability of PNA:DNA hybrids.

The intrinsically cationic amine- and guanidine-substituted PNAs were found to be efficient in cell permeability as seen by live cell imaging of NIH 3T3 and MCF-7 cells. The green fluorescence from the labeled PNAs (cationic and neutral *aeg*-PNA) was intense in the cytoplasm around the nuclear membrane. A similar effect was noticed by Sahu et al.[16] in the case of γ-substituted guanidino PNA (γGPNA) having 4 methylene spacers that localized within the vicinity of the nucleus, suspected to be in the endoplasmic reticulum, in HeLa cells. Thus, this feature seems to be a characteristic of cationic PNAs and may have potential utility in their antisense applications. Quantitation of cell permeation of PNAs by FACS analysis as well as estimating percentage of cells uptaking PNAs in both cell lines clearly established the superiority of cationic amino/guanidino PNAs in cell penetration, with 3−4-fold higher magnitude than unmodified PNAs.

CONCLUSIONS

Cationic PNA analogues are capable of enhancing the inherent cell permeability of PNAs. Comparative studies on cationic $C^{\gamma}(S)$-ethyleneamino- and $C^{\gamma}(S)$-ethyleneguanidino-substituted oligo PNA mixmers have shown their superior binding affinities toward complementary DNA and RNA compared to neutral *aeg*-PNA accompanied by high sequence specificity. The current results fill an important gap on the features of spacer chains bearing cationic substitutions at C^{γ} of PNA backbone on the duplex stability: a reduction of the carbon chain length carrying cationic substitutions increases the PNA:DNA duplex stability. The fluorescent analogues of the cationic PNAs are also endowed with a greater efficiency of cell uptake with localization in the vicinity of the nucleus. The results also suggest that the cell-penetrating abilities of C^{γ}-substituted PNAs depend on the nature of the cationic group, with guanidinium being better than the amino group. Thus, the cationic, chiral, and cell-permeable PNAs that have high DNA/RNA binding affinity and sequence selectivity provide an attractive platform for designing fresh PNA-based therapeutic and diagnostic agents. These PNA analogues are akin to the cationic peptides that are efficient cell-penetrating agents and have the potential to cartel the necessary features for both target inhibition and cell penetration.

EXPERIMENTAL SECTION

(*S*)-4-Amino-2-((*tert*-butoxycarbonyl)amino)butanoic Acid (2). A slurry of Boc-L-glutamine **1** (5 g, 20.3 mmol), EtOAc (24 mL), CH_3CN (24 mL), H_2O (12 mL), and iodobenzene diacetate (7.87 g, 24 mmol) was cooled and stirred at 16 °C for 30 min. The temperature was maintained at 20 °C for 4 h, cooled to 0 °C, and filtered. The solid residue was washed with EtOAc and dried in vacuum to obtain compound **2** (2.65 g, 60% yield). mp = 200−201 °C; R_f = 0.2 EtOAc/MeOH (50:50); $[\alpha]^{25}_D$ + 13.6 (*c* 0.5, methanol); IR (neat) 2976, 2900, 2832, 1740, 1692, 1645, 1563, 1546 cm^{-1}; ^1H NMR (400 MHz, CD_3OD) δ 4.04−4.01 (m, 1H), 2.98−2.94 (t, *J* = 8 Hz, 2H), 2.12−1.87 (m, 2H), 1.39 (s, 9H); ^{13}C NMR (100 MHz, CD_3OD) δ 176.3, 158.2, 80.9, 53.8, 38.3, 32.0, 28.8; HRMS (ESI-TOF) *m*/*z* calcd for $C_9H_{18}N_2O_4$ $[M + H]^+$ 219.1345, found 219.1342.

(*S*)-4-(((Benzyloxy)carbonyl)amino)-2-((*tert*-butoxycarbonyl)amino)butanoic acid (3). The solution of aq $NaHCO_3$ (2.3 g, 25 mL, 27 mmol) was added to an ice-cold solution of compound **2** (2 g, 9.2 mmol) in acetone (25 mL) and stirred for 10 min at 0 °C. To this, benzyl chloroformate (3.75 g, 3.7 mL, 11 mmol) in 50% toluene solution was added, and the reaction mixture was stirred overnight at room temperature. Acetone was removed; the aqueous layer was washed with Et_2O (2 × 20 mL), acidified to pH 2−3 with aq $KHSO_4$ (sat) solution, and extracted with EtOAc (3 × 50 mL). The combined organic extracts were dried over anhydrous Na_2SO_4, filtered, and concentrated to give compound **3** as a sticky oil (2.9 g, 90% yield). R_f = 0.67 EtOAc/MeOH (50:50); $[\alpha]^{25}_D$ − 9.2 (*c* 1, methanol); IR (neat) 2931, 2354, 2318, 1792, 1770, 1705, 1647, 1626 cm^{-1}; ^1H NMR (400 MHz, $CDCl_3$) δ 7.40−7.31 (m, 5H), 5.66−5.64 (m, 1H), 5.48−5.43 (m, 1H), 5.14−5.04 (m, 2H), 4.35−4.32 (m, 1H), 3.50−3.06 (m, 2H), 2.07−1.76 (m, 2H), 1.43 (s, 9H); ^{13}C NMR (100 MHz, $CDCl_3$) δ 175.7, 157.0, 156.0, 136.3, 128.5, 128.1, 80.3, 66.9, 51.1, 37.2, 33.3, 28.3; HRMS (ESI-TOF) *m*/*z* calcd for $C_{17}H_{24}N_2O_6$ $[M + Na]^+$ 375.1531, found 375.1531.

(*S*)-Methyl-4-(((benzyloxy)carbonyl)amino)-2-((*tert*-butoxycarbonyl)amino)butanoate (4). To a stirred solution of compound **3** (5.1 g, 14.5 mmol) in acetone (80 mL), K_2CO_3 (5 g, 36 mmol) was added followed by dimethyl sulfate (1.7 mL, 17.4 mmol). The reaction mixture was heated to 55 °C for 4 h under reflux condenser. Acetone was evaporated, and water (100 mL) was added to the concentrate, which was extracted with EtOAc (3 × 60 mL). The combined organic extracts were washed with brine, dried over anhydrous Na_2SO_4, filtered, and concentrated. The residue was purified on silica gel (60−120 mesh) using petroleum ether and EtOAc to give compound **4** as a white solid (5 g, 93% yield). mp = 67−69 °C; R_f = 0.5 petroleum ether/EtOAc (70:30); $[\alpha]^{25}_D$ − 18.8 (*c* 0.5, methanol); IR (neat) 3341, 2975, 1698, 1518, 1446 cm^{-1}; ^1H NMR (200 MHz, $CDCl_3$) δ 7.39−7.33 (m, 5H), 5.61 (br, 1H), 5.38 (app d, *J* = 8 Hz, 1H), 5.2−5.11 (m, 2H), 4.44−4.34 (m, 1H), 3.73 (s, 3H), 3.55−3.07 (m, 2H), 2.15−1.65 (m, 2H), 1.45 (s, 9H); ^{13}C NMR (50 MHz, $CDCl_3$) δ 172.9, 156.3, 155.7, 136.5, 128.3, 127.9, 80.0, 66.5, 52.3, 50.8, 37.0, 33.2, 28.1; HRMS (ESI-TOF) *m*/*z* calcd for $C_{18}H_{26}N_2O_6$ $[M + Na]^+$ 389.1688, found 389.1688.

dx.doi.org/10.1021/jo501639m | J. Org. Chem. 2014, 79, 9567−9577

(*S*)-Benzyl-*tert*-butyl (4-Hydroxybutane-1,3-diyl)-dicarbamate (5). To a stirred solution of compound **4** (5 g, 13.6 mmol) in absolute EtOH (60 mL) was added $NaBH_4$ (1.6 g, 41 mmol), and the reaction mixture was stirred for 6 h under N_2 atmosphere at room temperature. EtOH was evaporated completely, and water (100 mL) was added to the concentrate, which was extracted with EtOAc (3 × 60 mL). The combined organic extracts were washed with brine, dried over anhydrous Na_2SO_4, filtered, and concentrated. The residue was then purified on silica gel (60−120 mesh) using petroleum ether and EtOAc to give compound **5** as a white solid (4.1 g, 89% yield). mp = 80−82 °C; R_f = 0.4 petroleum ether/EtOAc (50:50); $[\alpha]^{25}_D$ − 24.4 (*c* 0.5, methanol); IR (neat) 3334, 2974, 1689, 1519, 1453 cm^{-1}; ^1H NMR (400 MHz, $CDCl_3$) δ 7.36−7.29 (m, 5H), 5.64 (br, 1H), 5.13−5.05 (m, 2H), 5.01 (br, 1H), 3.68−3.66 (app d, *J* = 8 Hz, 2H), 3.59−3.42 (m, 2H), 3.06−3.0 (m, 1H), 1.76−1.55 (m, 2H), 1.43 (s, 9H); ^{13}C NMR (100 MHz, $CDCl_3$) δ 155.6, 136.5, 128.4, 128.0, 79.7, 66.6, 65.2, 49.7, 37.6, 32.0, 28.3; HRMS (ESI-TOF) *m*/*z* calcd for $C_{17}H_{26}N_2O_5$ $[M + Na]^+$ 361.1739, found 361.1743.

(*S*)-4-(((Benzyloxy)carbonyl)amino)-2-((*tert*-butoxycarbonyl)amino)butyl Methanesulfonate (6). To an ice-cold solution of compound **5** (4 g, 12 mmol), Et_3N (4.18 mL, 30 mmol) in dry dichloromethane (DCM) (50 mL) was added mesyl chloride (1.21 mL, 15.6 mmol), and the reaction mixture was stirred for 30 min at 0 °C under N_2 atmosphere. To the reaction mixture DCM (20 mL) was added, and it was washed with water (40 mL) and brine (30 mL). The organic layer was dried over anhydrous Na_2SO_4, filtered, and concentrated to give compound **6** (4.5 g, 92% crude yield). R_f = 0.53 petroleum ether/EtOAc (50:50). This compound was used for the next step without further purification.

(*S*)-Benzyl-*tert*-butyl (4-Azidobutane-1,3-diyl)dicarbamate (7). A solution of compound **6** (4.5 g, 11 mmol) and NaN_3 (10.86 g, 165 mmol) in dry dimethylformamide (DMF) (50 mL) was heated to 80 °C for 8 h. To the reaction mixture water (100 mL) was added, which was extracted with EtOAc (3 × 70 mL). The ethyl acetate layer was washed with water (50 mL) and brine (50 mL). The combined organic extracts were dried over anhydrous Na_2SO_4, filtered, and concentrated. The residue obtained was then purified on silica gel (60−120 mesh) using petroleum ether and EtOAc to give compound **7** as a sticky yellowish oil (3.53 g, 87% yield). R_f = 0.73 petroleum ether/EtOAc (50:50); $[\alpha]^{25}_D$ − 33.6 (*c* 1, methanol); IR (neat) 3332, 2974, 2931, 2098, 1691, 1517 cm^{-1}; ^1H NMR (400 MHz, $CDCl_3$) δ 7.32−7.28 (m, 5H), 5.53 (br, 1H), 5.09−5.01 (m, 2H), 4.82 (br, 1H), 3.80−3.76 (m, 1H), 3.45−3.38 (m, 2H), 3.35−2.97 (m, 2H), 1.68−1.50 (m, 2H), 1.40 (s, 9H); ^{13}C NMR (100 MHz, $CDCl_3$) δ 156.4, 155.7, 136.5, 128.4, 128.0, 19.8, 66.5, 54.9, 47.6, 37.4, 32.8, 28.1; HRMS (ESI-TOF) *m*/*z* calcd for $C_{17}H_{25}N_5O_4$ $[M + Na]^+$ 386.1804, found 386.1802.

(*S*)-Ethyl-2-((4-(((benzyloxy)carbonyl)amino)-2-((*tert*-butoxycarbonyl)amino)butyl)amino)acetate (8). To a solution of compound **8** (750 mg, 2.0 mmol) in absolute EtOH (15 mL) was added Raney Ni (2 mL). The reaction mixture was hydrogenated in a Parr apparatus for 6 h at room temperature and H_2 pressure of 50−55 psi. The reaction mixture was filtered to remove catalyst, and the solvent was removed under reduced pressure to yield a residue of free amine (626 mg) as yellowish oil that was taken in CH_3CN (20 mL). To this, Et_3N (0.8 mL, 5.5 mmol) was added and stirred at 0 °C for 10 min, and ethylbromo acetate (0.18 mL, 1.7 mmol) was added dropwise followed by keeping the reaction mixture stirred for 12 h at room temperature. CH_3CN was evaporated, and water (50 mL) was added to the concentrate. The aqueous layer was extracted with EtOAc (3 × 40 mL), and the combined organic extracts were washed with aq $NaHCO_3$ (sat) and brine, dried, and concentrated. The residue obtained was purified on silica gel (100−200 mesh) using petroleum ether and EtOAc to give compound **8** as a yellowish oil (700 mg, 80%). R_f = 0.48 petroleum ether/EtOAc (20:80); $[\alpha]^{25}_D$ − 10.4 (*c* 1, methanol); IR (neat) 3329, 2929, 2354, 2318, 1738, 1705, 1694, 1647, 1529, 1516 cm^{-1}; ^1H NMR (200 MHz, $CDCl_3$) δ 7.25−7.20 (m, 5H), 5.76 (br, 1H), 5.06−4.93 (m, 3H), 4.14−4.03 (q, *J* = 8 Hz, 2H), 3.65−3.63 (m, 1H), 3.42−3.22 (m, 3H), 2.95−2.86 (m, 1H), 2.71−2.55 (m, 3H), 1.64−1.42 (m, 2H), 1.34 (s, 9H), 1.21−1.14 (t, *J* = 7 Hz, 3H); ^{13}C NMR (50 MHz, $CDCl_3$) δ 171.9, 156.4, 136.6, 128.3, 127.9, 127.8, 79.4, 66.3, 60.8, 52.8, 50.4, 47.5, 37.4, 33.5, 29.5, 28.2, 14.0; HRMS (ESI-TOF) *m*/*z* calcd for $C_{21}H_{33}N_3O_6$ $[M + H]^+$ 424.2447, found 424.2444.

(*S*)-Ethyl-2-(*N*-(4-(((benzyloxy)carbonyl)amino)-2-((tert-butoxycarbonyl)amino)butyl)-2-chloroacetamido)acetate (9). To an ice-cold solution of compound **8** (3.1 g, 7.3 mmol) in dry DCM (50 mL) and Et_3N (2.96 g; 4 mL, 29.2 mmol) was added chloroacetyl chloride (0.82 g; 0.58 mL, 7.3 mmol), and the reaction mixture was stirred for 8 h. The reaction mixture was diluted with DCM (20 mL) and washed with water (60 mL) and brine (60 mL). The organic layer was dried over anhydrous Na_2SO_4, filtered, and concentrated. The residue was purified on silica gel (100−200 mesh) using petroleum ether and EtOAc to give compound **9** as a colorless sticky oil (2.63 g, 72%). R_f = 0.59 petroleum ether/EtOAc (40:60); $[\alpha]^{25}_D$ − 10.8 (*c* 1, methanol); IR (neat) 3335, 2977, 2934, 1698, 1657, 1519, 1454, 1368 cm^{-1}; ^1H NMR (200 MHz, $CDCl_3$) δ 7.337.26 (m, 5H), 5.61 (maj) 5.35 (min) (br, 1H), 5.15−5.0 (m, 2H), 4.27−4.12 (m, 4H), 3.99 (s, 2H), 3.88−3.65 (m, 2H), 3.52−3.38 (m, 2H), 3.25−2.95 (m, 2H), 1.70−1.64 (m, 2H), 1.41 (min) 1.40 (maj) (s, 9H), 1.31−1.21 (m, 3H); ^{13}C NMR (50 MHz, $CDCl_3$) δ 169.1, 168.7, 168.3, 167.4, 156.5, 136.5, 128.4, 127.9, 79.4, 66.4, 62.0, 61.4, 52.8, 50.7, 49.8, 48.6, 46.8, 40.9, 37.3, 33.1, 32.3, 28.2, 14.0; HRMS (ESI-TOF) *m*/*z* calcd for $C_{23}H_{34}ClN_3O_7$ $[M + Na]^+$ 522.1982, found 522.1985.

(*S*)-Ethyl-2-(*N*-(4-(((benzyloxy)carbonyl)amino)-2-((*tert*-butoxycarbonyl)amino)butyl)-2-(5-methyl-2,4-dioxo-3,4-dihydropyrimidin-1(2H)-yl)acetamido)acetate (10). A solution of compound **9** (1 g, 2 mmol) in dry DMF (20 mL) containing K_2CO_3 (0.33 g, 2.4 mmol) and thymine (0.3 g, 2.4 mmol) was stirred at room temperature for 12 h. To the reaction mixture water (40 mL) was added and extracted with EtOAc (3 × 50 mL), and the organic layer was washed with water (50 mL) and brine (30 mL). The combined organic extracts were dried over anhydrous Na_2SO_4, filtered, and concentrated. The residue obtained was purified on silica gel (100−200 mesh) using petroleum ether and EtOAc to give compound **10** as a white solid (0.95 g, 81%). mp = 92−94 °C; R_f = 0.47 EtOAc; $[\alpha]^{25}_D$ − 8.1 (*c* 1, methanol); IR (neat) 3332, 2978, 1671, 1519, 1464, 1369 cm^{-1}; ^1H NMR (400 MHz, $CDCl_3$) δ 9.86 (maj) 9.56 (min) (br, 1H), 7.37−7.27 (m, 5H), 7.05 (min) 6.98 (maj) (s, 1H), 5.67−5.63 (maj) 5.58−5.56 (min) (comp, 1H), 5.11−5.04 (m, 2H), 4.82 (min) 4.78 (maj) (br, 1H), 4.47−4.37 (m, 1H), 4.28−4.13 (m, 3H), 3.94−3.51 (m, 3H), 3.43−3.02 (m, 3H), 2.17 (br, 1H), 1.89 (min) 1.87 (maj) (s, 3H), 1.69−1.67 (comp, 1H), 1.41 (maj) 1.39 (min) (s, 9H), 1.31−1.23 (m, 3H); ^{13}C NMR (100 MHz, $CDCl_3$) δ 169.1, 167.5, 164.4, 156.7, 151.5, 140.9, 136.5, 128.4, 128.0, 110.8, 79.6, 66.6, 62.3, 52.1, 51.5, 49.8, 48.6, 47.8, 47.2, 37.6, 32.9, 28.3, 14.0, 12.3; HRMS (ESI-TOF) *m*/*z* calcd for $C_{28}H_{39}N_5O_9$ $[M + Na]^+$ 612.2645, found 612.2646.

(*S*)-2-(*N*-(4-(((Benzyloxy)carbonyl)amino)-2-((*tert*-butoxycarbonyl)amino)butyl)-2-(5-methyl-2,4-dioxo-3,4-dihydropyrimidin-1(2*H*)-yl)acetamido)acetic Acid (11). To a stirred solution of compound **10** (500 mg, 0.8 mmol) in MeOH was added aq LiOH (10%), and the reaction mixture was stirred for 3 h at room temperature. MeOH was removed under vacuum, and the aqueous layer was washed with diethyl ether and neutralized with activated Dowex H^+ to pH ≈ 4−5. The resin was removed by filtration, and the filtrate was concentrated to obtain the resulting compound **11** as a white solid (0.42 g, 88%). mp = 241−245 °C; R_f = 0.5 EtOAc/MeOH (50:50); $[\alpha]^{25}_D$ − 3.0 (*c* 0.5, methanol); IR (neat) 3341, 2938, 2354, 2317, 1728, 1678, 1537, 1474, 1441, 1369 cm^{-1}; ^1H NMR (400 MHz, DMSO-d^6) δ 11.30 (min) 11.25 (maj) (br, 1H), 7.35−7.26 (m, 5H), 7.21−7.15 (m, 1H), 6.91−6.89 (min) 6.78−6.76 (maj) (d, *J* = 8 Hz, 1H), 5.02−4.96 (m, 2H), 4.76−4.72 (maj) 4.59−4.55 (min) (d, J = 16 Hz, 1H), 4.42 (s, 2H), 3.97−3.74 (m, 4H), 3.47−3.21 (m, 2H), 3.12−2.91 (m, 3H), 1.75 (min) 1.73 (maj) (s, 3H), 1.58−1.41 (m, 2H), 1.37 (maj) 1.36 (min) (s, 9H); ^{13}C NMR (100 MHz, $CDCl_3$) δ 170.6, 167.9, 167.0, 164.5, 156.0, 155.5, 151.1, 142.1,137.3, 108.0, 77.7, 65.1, 51.9, 51.1, 48.4, 47.7, 47.1, 46.5, 37.7, 32.1, 28.3, 12.0; HRMS (ESI-

dx.doi.org/10.1021/jo501639m | J. Org. Chem. 2014, 79, 9567−9577

TOF) m/z calcd for $C_{26}H_{35}N_5O_9$ $[M + Na]^+$ 584.2332, found 584.2335.

(*S*)-Ethyl-5-(((Benzyloxy)carbonyl)amino)-9-((*tert*-butoxycarbonyl)amino)-11-(2-(5-methyl-2,4-dioxo-3,4-dihydropyrimidin-1(2*H*)-yl)acetyl)-3-oxo-1-phenyl-2-oxa-4,6,11-triazatridec-4-en-13-oate (12). To a solution of compound **10** (1 g, 1.7 mmol) in absolute EtOH (10 mL) was added 10% Pd/C (100 mg) and a catalytic amount of glacial acetic acid (50 μL). The reaction mixture was subjected to hydrogenation on a Parr hydrogenator at 60 psi for 12 h, after which it was filtered and concentrated to get free amine (0.76 g, 1.7 mmol). It was taken in dry DMF (10 mL) to which *N*,*N*′-bis-di-Cbz-S-Me isothiourea (0.62 g, 1.7 mmol) and a catalytic amount of 4-dimethylaminopyridine (DMAP) were added under N_2 atmosphere. The reaction mixture was stirred for 12 h at room temperature; water (20 mL) was added and extracted with EtOAc (3 × 40 mL). The combined organic extracts were washed with water (40 mL) and brine (30 mL). The organic layer was dried over anhydrous Na_2SO_4, filtered, and concentrated under reduced pressure. The residue obtained was then purified on silica gel (100−200 mesh) using petroleum ether and EtOAc to give compound **12** as a white solid (0.93 g, 72% yield). mp = 99−102 °C; R_f = 0.48 EtOAc; $[\alpha]^{25}_D$ − 1.1 (*c* 1, methanol); IR (neat) 3332, 2977, 1675, 1638, 1573, 1507, 1451, 1427, 1376, 1323 cm^{-1}; ^1H NMR (400 MHz, $CDCl_3$) δ 11.70 (s, 1H), 9.24 (br, 1H), 8.52−8.51 (app d, J = 4 Hz, 1H), 7.39−7.28 (m, 10H), 7.02 (min) 6.98 (maj) (s, 1H), 5.78 (d, J = 8 Hz, 1H), 5.22−5.09 (m, 4H), 4.84−4.80 (app d, J = 16 Hz, 1H), 4.45−4.13 (m, 5H), 3.96−3.69 (m, 2H), 3.64−3.31 (m, 4H), 2.09 (br, 1H), 1.90 and 1.88 (s, 3H), 1.82−1.58 (m, 2H), 1.41 (maj) 1.38 (min) (s, 9H), 1.30 (min) 1.25 (maj) (t, J = 8 Hz, 3H); ^{13}C NMR (100 MHz, $CDCl_3$) δ 169.1, 168.4, 167.5, 164.2, 163.5, 156.1, 153.6, 151.2, 141.1, 136.6, 134.5, 128.8, 128.4, 128.0, 110.6, 79.8, 68.2, 67.1, 62.2, 61.4, 52.2, 51.3, 50.0, 48.8, 47.7, 37.9, 31.9, 28.3, 14.0, 12.3; HRMS (ESI-TOF) m/z calcd for $C_{37}H_{47}N_7O_{11}$ $[M + H]^+$ 766.3412, found 766.3403.

(*S*)-5-(((Benzyloxy)carbonyl)amino)-9-((*tert*-butoxycarbonyl)amino)-11-(2-(5-methyl-2,4-dioxo-3,4-dihydropyrimidin-1(2*H*)-yl)acetyl)-3-oxo-1-phenyl-2-oxa-4,6,11-triazatridec-4-en-13-oic Acid (13). To a stirred solution of compound **12** (0.5 g, 0.65 mmol) in tetrahydrofuran (THF) was added aq NaOH (2 N, 4 mL) at 0 °C, and the reaction mixture was stirred for 30 min at 0 °C. THF was evaporated, and the aqueous layer was washed with EtOAc (2 × 20 mL). The aqueous layer was neutralized with 5 N HCl at 0 °C to pH 3−4 and extracted with EtOAc (3 × 30 mL). The combined organic extracts were dried over anhydrous Na_2SO_4, filtered, and evaporated to give compound **13** as a white solid (0.37 g, 78% yield). mp = 95−97 °C; R_f = 0.73 EtOAc/MeOH (50:50); $[\alpha]^{25}_D$ + 3.7 (*c* 1, methanol); IR (neat) 3339, 2923, 2852, 2354, 2317, 1728, 1671, 1632, 1525, 1423, 1363, 1325, 1254 cm^{-1}; ^1H NMR (400 MHz, $CDCl_3$) δ 11.74 (br, 1H), 10.10 (br, 1H), 8.53 (br, 1H), 7.37−7.28 (m, 10H), 6.99 (s, 1H), 6.62 (s, 1H), 5.76 (br, 1H), 5.30−5.10 (m, 5H), 4.70−4.01 (m, 4H), 3.80−3.29 (m, 6H), 1.85 (maj) 1.82 (min) (s, 3H), 1.40 (min) 1.38 (maj) (s, 9H); ^{13}C NMR (100 MHz, $CDCl_3$) δ 170.9, 170.5, 168.0, 167.4, 164.4, 163.1, 155.7, 155.2, 152.7, 151.0, 141.8, 136.9, 135.2, 128.6, 128.4, 128.1, 127.9, 126.7, 126.5, 115.7, 108.2, 78.2, 67.6, 66.4, 62.9, 51.1, 47.7, 46.9, 39.5, 38.0, 34.4, 31.0, 30.5, 28.2, 28.2, 12.0; HRMS (ESI-TOF) m/z calcd for $C_{35}H_{43}N_7O_{11}$ $[M + H]^+$ 738.3099, found 738.3092.

Solid-Phase Synthesis Protocol. The modified and unmodified PNA monomers were incorporated into 10-mer PNA sequence by solid-phase synthesis on L-lysine-derivatized MBHA resin (50 mg) having 0.35 mmol/g loading value. The solid-phase synthesis was carried out in a glass sintered flask. The deprotection of N-*t*-*Boc* group from the resin-bound lysine with 50% TFA in DCM (3 × 15 min) was followed by washing with DCM and DMF (3 × 10 mL) to give a TFA salt of amine, which was neutralized using 10% *N*,*N*-diisopropylethylamine (DIPEA) in DCM (3 × 10 min) to liberate free amine. After washing with DCM and DMF (3 × 10 mL), the free amine was coupled with carboxylic acid of the incoming monomer (A/T/G/C; 3 equiv) in DMF (500 μL) using HOBt (3 equiv), HBTU (3 equiv), and DIPEA (3 equiv). The reagents were then removed by filtration, and the resin was washed with DMF.

Purification of PNA Oligomers by Reverse-Phase HPLC. For the purification of peptides, a semipreparative BEH130 C18 (10 × 250 mm) column was used. Purification of PNA oligomers was performed with the gradient elution method: A to 100% B in 20 min; A = 0.1% TFA in CH_3CN/H_2O (5:95); B = 0.1% TFA in CH_3CN/H_2O (1:1) with a flow rate of 3 mL/min. Control *aeg*-, *eam*-, and *egd*-modified PNA oligomers were monitored at 254 nm wavelength, while all fluorescent PNA oligomers were monitored at both 254 and 490 nm wavelengths.

UV−T_m Measurements. UV−melting experiments were carried out on a UV-spectrophotometer equipped with a Peltier heater. The samples for T_m measurement were prepared by mixing the calculated amounts of respective oligonucleotides in a stoichiometric ratio (1:1) in sodium phosphate buffer (10 mM, pH 7.2) containing ethylenediaminetetraacetic acid (EDTA) (0.1 mM) and NaCl (10 mM) to a final concentration of 2 μM for each strand. The samples were annealed by heating at 90 °C for 3 min followed by slow cooling to room temperature for at least 6−8 h and then being refrigerated for at least 4−5 h. The samples (500 μL) were transferred to a quartz cell and equilibrated at the starting temperature for 2 min. The optical density (OD) at 260 nm was recorded in steps from 20 to 85 °C with a temperature increment of 1 °C/min. Each melting experiment was repeated at least twice. The normalized absorbance at 260 nm was plotted as a function of the temperature. The T_m was determined from the first derivative of normalized absorbance with respect to temperature and is accurate to ±0.5 °C. The data were processed using Microcal Origin 8.0/8.5. The concentrations of all oligonucleotides were calculated on the basis of absorbance from the molar extinction coefficients of the corresponding nucleobases, i.e., T = 8.8; C = 7.3; G = 11.7; and A = 15.4 $cm^2/\mu mol$.

Circular Dichroism Studies. CD spectra were recorded on a spectropolarimeter connected with a Peltier heater. The calculated amounts of PNA oligomers and the complementary DNA **1** were mixed together in 1:1 stoichiometry in sodium phosphate buffer (10 mM, pH 7.2) containing EDTA (0.1 mM) and NaCl (10 mM) to achieve a final concentration of 5 μM for each strand. The samples were annealed by heating at 90 °C for 3 min followed by slow cooling to room temperature for at least 6−8 h. The cooled samples were transferred to a refrigerator for at least 4−5 h. The CD spectra of PNA:DNA, PNA:RNA duplexes, and single-stranded PNAs were recorded at 10 °C with an accumulation of five scans from 300 to 190 nm using a 2 mm cell, a resolution of 0.1 nm, a bandwidth of 1 nm, a sensitivity of 2 m deg, a response of 2 s, and a scan speed of 50 nm/min.

Ethidium Bromide Displacement Assay from ds-DNA. Calculated amounts of complementary DNA strands (1:1) were annealed to get DNA duplex (2 μM, 400 μL) in the sodium phosphate buffer (pH 7.2). Aliquots (1 μL) of EtBr (250 μM) were added to the annealed samples, and the fluorescence intensity at 610 nm was recorded until it got saturated. The resulting EtBr−ds-DNA complex was titrated against individual PNA oligomers in the aliquots of 0.4 μL, and the change in fluorescence emission at 610 nm was recorded. The percent change observed in fluorescence intensity (I/I_0) upon displacement of EtBr was plotted against the concentration of PNA oligomers using Microcal Origin 8.5.

Electrophoretic Mobility Shift Assay and Competition Binding Experiment. The calculated amounts of PNA oligomers (3 nmol) were individually mixed with DNA strands (3 nmol) in 1:1 ratio in sodium phosphate buffer (10 mM, NaCl 100 mM, pH 7.2; 10 μL). The samples were annealed by heating to 90 °C for 3 min followed by slow cooling to RT and refrigeration at 4 °C overnight. To this, 5 μL loading buffer (10 mM Tris-HCl, pH 8; 30% sucrose and 10% glycerol) was added, and samples were loaded on the gel. Bromophenol blue (BPB) was used as the tracer dye and separately loaded in an adjacent well. Gel electrophoresis was performed on 20% nondenaturing polyacrylamide gel (acrylamide/*N*,*N*′-methylenebis-(acrylamide), 19:1) with 1X-TBE containing 500 mM NaCl as the tank buffer at a constant power supply of 14 W and 120 V for 30 h. During electrophoresis, the temperature was maintained at ∼18 °C.

dx.doi.org/10.1021/jo501639m | J. Org. Chem. 2014, 79, 9567−9577

The spots were visualized through UV shadowing by illuminating the gel placed on a fluorescent silica gel plate, F254 using UV light.

Cellular Uptake Experiment using Confocal Microscopy. MCF-7 and NIH 3T3 cells were plated in 8-well chambered cover glass in 200 μL of Dulbecco's modified Eagle medium (DMEM) containing 10% fetal bovine serum (FBS) at the concentration of 8000 cells per well. The cells were grown by maintaining at 37 °C in a humidified atmosphere containing 5% CO_2 for 16 h. The required amounts of 5(6)-carboxyfluorescein tagged PNA stock solutions were added to the corresponding wells to achieve the desired final concentration of 1 μM. The cells incubated with tagged PNA oligomers were maintained at 37 °C in a humidified atmosphere containing 5% CO_2 for 24 h. After the incubation period was over, the medium was aspirated and the cells were rinsed or washed thrice with 1 medium-volume equivalent of 1X phosphate-buffered saline (PBS). The cells were then replenished with 400 μL of OPTIMEM medium containing Hoechst 33342 at a dilution of 1/1000 of the supplied stock solution (10 mg/mL) and left for 15 min at 37 °C. After incubation for 15 min, the medium containing nuclear stain Hoechst 33342 was removed and rinsed with 1X PBS and replenished with fresh OPTIMEM medium. The cells were then immediately visualized using 40× objective of a laser scanning confocal microscope. Cells incubated with 5(6)-carboxyfluorescein including unmodified *aeg*-PNA were used as control. The results are indicative of two independent biological replicates.

Quantification of Cellular Uptake by FACS Analysis. MCF-7 and NIH 3T3 cells were plated in 9 × 60 mm dishes in 2 mL of DMEM medium at a concentration of 1×10^6 cells per dish. The cells were maintained at 37 °C in a humidified atmosphere containing 5% CO_2 for 16−18 h. The required amounts of 5(6)-carboxyfluorescein-tagged PNA stock solutions were added to the corresponding wells to achieve the desired final concentration of 1 μM. The cells incubated with tagged PNA oligomers were maintained at 37 °C in a humidified atmosphere containing 5% CO_2 for 24 h. After the incubation period was over, the medium was aspirated and the cells were rinsed or washed thrice with 1 medium-volume equivalent of ice-cold PBS. Cells were collected by trypsinization using 0.5 mL of 0.05% trypsin−EDTA for each dish. The trypsinization process was stopped by using 3 mL of DMEM medium, and the cells were transferred to 15 mL tubes. These tubes containing cells were centrifuged at 150*g* for 5 min at 4 °C; the supernatant was aspirated, and the cells were washed thrice with ice-cold 1X PBS. The cell suspension in PBS was then transferred to a FACS tube, and the samples were immediately analyzed on flow cytometer. The data obtained from FACS were processed using CellQuest Pro software. The cell permeation of PNA oligomers has been confirmed by histograms obtained from the experiment. The percent positive cells for each individual PNA were plotted on Microcal Origin 8.

Cytotoxicity (MTT) Assay. NIH 3T3 cells were cultivated in DMEM medium supplemented with 10% fetal calf serum (FCS) and 1% penicillin−streptomycin. Cells were harvested for use by removing culture media and adding trypsin (1 mL) to the culture flask to release the cells from the wall of the dish. Ten percent fetal bovine serum (FBS) media (1 mL) was added to quench the trypsin. The cells were suspended in solution, centrifuged (1000 rpm, 5 min), and diluted to a concentration of 10^4 cells per 100 mL media. Cells were allotted to the wells of a 96-well plate (10^4 cells or 100 mL per well), and carboxyfluorescein-tagged PNA oligomers were incubated at 37 °C for 24 h in various concentrations (0.5−2 μM). The well containing only medium was used as a positive control for cell death. After incubation, 3-(4,5-dimethylthiazol-2-yl)-2,5-diphenyltetrazolium bromide (MTT; 50 mL of 2.5 g/L in PBS) was added and cells were incubated for an additional 4 h. The supernatant was removed, and the precipitated crystals were dissolved in 100 μL of dimethylsulfoxide (DMSO). The absorbance of this solution was measured at 570 nm and referenced to the blank wells to find the relative cell viabilities for each assay condition.

■ ASSOCIATED CONTENT

Supporting Information

^{1}H NMR and ^{13}C NMR spectra of intermediate compounds **2**−**13**; HPLC and MALDI-TOF spectra of PNA oligomers (PNA **1**−**10** and fluorescent PNAs); UV-melting profiles of various PNA:DNA and PNA:RNA duplexes; CD spectra of all single-stranded PNAs and duplexes of modified PNAs with DNA **1** and RNA **1**; EtBr displacement by various PNAs; confocal images of various fluorescently labeled PNAs and FACS analysis in MCF-7 cells; MTT assay in NIH 3T3 cells. This material is available free of charge via the Internet at http://pubs.acs.org.

■ AUTHOR INFORMATION

Corresponding Author

*Tel.: 91 (20) 2590 8021. Fax: 91 (20) 2589 9790. E-mail: kn.ganesh@iiserpune.ac.in.

Notes

The authors declare no competing financial interest.

■ ACKNOWLEDGMENTS

D. R. J. acknowledges IISER Pune for award of a research fellowship. L. A. V. acknowledges INSPIRE-DST for award of fellowship. K. N. G. is a recipient of the JC Bose Fellowship, Department of Science and Technology, New Delhi. We thank the Director of NCCS, Pune, for assistance and helpful discussion in FACS analysis.

■ REFERENCES

(1) Nielsen, P. E.; Egholm, M.; Berg, R. H.; Buchardt, O. *Science* **1991**, *254*, 1497−1500.
(2) Egholm, M.; Buchardt, O.; Nielsen, P. E.; Berg, R. H. *J. Am. Chem. Soc.* **1992**, *114*, 1895−1897.
(3) Egholm, M.; Buchardt, O.; Christensen, L.; Behrens, C.; Freier, S. M.; Driver, D. A.; Berg, R. H.; Kim, S. K.; Norden, B.; Nielsen, P. E. *Nature* **1993**, *365*, 566−568.
(4) Jensen, K. K.; Qrum, H.; Nielsen, P. E.; Norden, B. *Biochemistry* **1997**, *36*, 5072−5077.
(5) Nielsen, P. E. *Acc. Chem. Res.* **1999**, *32*, 624−630.
(6) Nielsen, P. E. *Mol. Biotechnol.* **2004**, *26*, 233−248.
(7) Nielsen, P. E.; Egholm, M.; Berg, R. H.; Buchardt, O. *Anti-Cancer Drug Des.* **1993**, *8*, 53−63.
(8) Nielsen, P. E. *Q. Rev. Biophys.* **2005**, *38*, 345−350.
(9) Ganesh, K. N.; Nielsen, P. E. *Curr. Org. Chem.* **2000**, *4*, 931−943.
(10) Kumar, V. A.; Ganesh, K. N. *Acc. Chem. Res.* **2005**, *38*, 404−412.
(11) Kumar, V. A.; Ganesh, K. N. *Curr. Top Med. Chem.* **2007**, *7*, 715−726.
(12) Haaima, G.; Lohse, A.; Buchardt, O.; Nielsen, P. E. *Angew. Chem., Int. Ed.* **1996**, *35*, 1939−1942.
(13) Sforza, S.; Corradini, R.; Ghirardi, S.; Dossena, A.; Marchelli, R. *Eur. J. Org. Chem.* **2000**, 2905−2913.
(14) Menchise, V.; Simone, G. D.; Tedeschi, T.; Corradini, R.; Sforza, S.; Marchelli, R.; Capasso, D.; Saviano, M.; Pedone, C. *Proc. Natl. Acad. Sci. U. S. A.* **2003**, *100*, 12021−12026.
(15) Dragulescu-Andrasi, A.; Zhou, P.; He, G.; Ly, D. H. *Chem. Commun.* **2005**, 244−246.
(16) Sahu, B.; Chenna, V.; Lathrop, K. L.; Thomas, S. M.; Zon, G.; Livak, K. J.; Ly, D. H. *J. Org. Chem.* **2009**, *74*, 1509−1516.
(17) Dragulescue-Andrasi, A.; Rapireddy, S.; Freeza, B. M.; Gayathri, C.; Gil, R. R.; Ly, D. H. *J. Am. Chem. Soc.* **2006**, *128*, 10258−10267.
(18) Sahu, B.; Sacui, I.; Rapireddy, S.; Zanotti, K. J.; Bahal, B.; Armitage, B. A.; Ly, D. H. *J. Org. Chem.* **2011**, *76*, 5614−5627.
(19) Sahu, B.; Sacui, I.; Rapireddy, S.; Zanotti, K. J.; Bahal, R.; Armitage, B. A.; Ly, D. H. *J. Org. Chem.* **2011**, *76*, 5614−5627.
(20) Jain, D. R.; Ganesh, K. N. *J. Org. Chem.* **2014**, *79*, 6708−6714.

(21) Mitra, R.; Ganesh, K. N. *Chem. Commun.* **2011**, *47*, 1198−1200.
(22) Mitra, R.; Ganesh, K. N. *J. Org. Chem.* **2012**, *77*, 5696−5707.
(23) Zhang, L. H.; Kauffman, G. S.; Pesti, J. A.; Yin, J. *J. Org. Chem.* **1997**, *62*, 6918−6920.
(24) Koch, T. PNA Synthesis by Boc Chemistry. In *Peptide Nucleic Acids: Protocols and Applications*, 2nd ed.; Nielsen, P. E., Ed.; Horizon Scientific Press: Norfolk, U.K., 2004; pp 37−59.
(25) Christensen, L.; Fitzpatrick, R.; Gildea, B.; Petersen, K.; Hansen, H. F.; Koch, C.; Egholm, M.; Buchardt, O.; Nielsen, P. E.; Coull, J.; Berg, R. H. *J. Peptide Sci.* **1995**, *3*, 175−183.
(26) Yeung, B. K. S.; Tse, W. C.; Boger, D. L. *Bioorg. Med. Chem. Lett.* **2003**, *13*, 3801−3804.
(27) Tse, W. C.; Boger, D. L. *Acc. Chem. Res.* **2004**, *37*, 61−69.
(28) Wittung, P.; Kim, S. K.; Buchardt, O.; Nielsen, P. E.; Norden, B. *Nucleic Acids Res.* **1994**, *22*, 5371−5377.
(29) Sambrook, J.; Fritsch, E. F.; Maniatis, T. In *Molecular Cloning: A Laboratory Manual 2*; Cold Spring Harbor Laboratory Press:Cold Spring Harbor, NY, 1989.
(30) Govindraju, T.; Kumar, V. A.; Ganesh, K. N. *J. Org. Chem.* **2004**, *69*, 1858−1865.
(31) Sugiyama, T.; Kittaka, A. *Molecules* **2013**, *18*, 287−310.
(32) Enguld, E. A.; Appella, D. H. *Angew. Chem., Int. Ed.* **2007**, *46*, 1414−1418.
(33) Manicardi, A.; Calabretta, A.; Bencivenni, M.; Tedeschi, T.; Sforza, S.; Corradini, R.; Marchelli, R. *Chirality* **2010**, *22*, 161−172.